The use of a colour camera for quantitative detection of protein-binding nanoparticles

Felicia Ungureanu[1], Jan Halamek, Remco Verdoold, Rob P.H. Kooyman

University of Twente, MESA+ Institute, Biophysical Engineering Group
P.O. Box 217; 7500 AE Enschede, the Netherlands

ABSTRACT

Metal nanoparticles posses the property of changing their optical properties as a function of both internal characteristics (size, shape, dielectric function) and refractive index of the local environment. A special class of applications in the field of biosensing uses the dependency of the nanoparticle's plasmonic peak localization on the local refractive index change. The response of this type of sensors is usually monitored by the change of the extinction spectrum of an ensemble of nanoparticles where analytes interact with functionalized nanoparticles in solution or immobilized at an interface; detection is done with a spectrophotometer. This type of sensors has a limited sensitivity. This can be overcome by using *single* nanoparticle based biosensors. This type of sensors measures the changes of the scatter spectrum of a collection of individually addressable functionalized nanoparticles in the presence of analytes.

Here we report on a new detection method of binding events of analytes to functionalized gold nanoparticle using a standard colour camera attached to a darkfield microscopy setup. This setup is capable of parallel detection of the spectral shifts of thousands of 60 nm antibody-functionalized gold spheres as a result of binding events of protein analyte molecules. This setup can be the basis for multiplexing and quantification.

Keywords: gold nanoparticles, darkfield microscopy, colour camera, protein quantification

1. INTRODUCTION

Often, the design of biosensing devices involves the use of optical reporters, such as colorimetric, fluorometric or chemiluminescent, either as direct or indirect labels [1, 2]. A common measuring approach is to obtain the cumulative signal of an ensemble of labels present in the region of interest. In such a system the detection of (nearly-) single molecule binding events is essentially impossible. This circumstance is one of the reasons why the ultimate sensitivity of such a 'macro-device' will be limited. An alternative to this approach is the detection of individual binding events using fluorescent labels. Yet, the low quantum yield, blinking, quenching and the irreversible photodestruction of the fluorescent molecules make single binding events difficult to detect, even if expensive equipment is used.

A new class of materials, noble metal nanoparticles, potentially overcomes these limitations. When such a particle is placed in an electromagnetic field with a certain well-defined resonant wavelength, a localized surface plasmon (a collective oscillation of the metal's free electrons) can be excited. In these conditions the scattering cross-section for a single 60 nm Au particle at a wavelength of 540 nm is around $2*10^{-20}m^2$, while the scattering cross-section of a fluorescein molecule is 10^5 smaller. This allows the visualization of single nanoparticles in e.g. a darkfield microscope, using relatively simple detection equipment.

The wavelength at which a surface plasmon can be excited in the nanoparticle is highly dependent on its intrinsic properties (composition, size, shape) as well as on the refractive index of the immediate environment [3]. It is this last property that makes nanoparticles interesting for biosensing. Okamoto et al [4] were the first to show the feasibility of a gold nanoparticles covered glass substrate as a stand-alone sensing platform for the monitoring of molecular binding in real time.

[1] f.ungureanu@tnw.utwente.nl ; phone: +31-(0)53-489 3163; 31-(0)53-489 1105, http://bpe.tnw.utwente.nl/

Plasmonics in Biology and Medicine VI, edited by Tuan Vo-Dinh, Joseph R. Lakowicz
Proc. of SPIE Vol. 7192, 71920O · © 2009 SPIE · CCC code: 1605-7422/09/$18 · doi: 10.1117/12.806522

Another important advantage of single nanoparticle sensor systems is the possibility of wavelength multiplexing. Unique sensing platforms can be fabricated by controlling the size, shape and chemical modification; each type can be distinguished from the other ones, based on their unique wavelength dependent scatter maxima [5].

The most common method of characterizing binding events on individual particles is resonant Rayleigh scattering spectroscopy [6-8]. For example, the method used by Sannomiya et al [9] for detecting individual binding event or single nanoparticles involves the use of a regular spectrometer attached to a microscope and scanning electron microscopy (SEM) for visual verification. Baciu et al [10], for the detection of streptavidin binding to membrane-coated particles, used, instead of a spectrometer an electronically addressable liquid crystal device, which gives them the advantage of simultaneously collecting the signal from several nanoparticles.

However, in view of the large number of nanoparticles present on the surface, which can undergo binding events, this detection method cannot be considered for quantification purposes.

In this paper we propose an alternate detection method by employing a colour camera in a quantitative way Its main advantages are (1) parallel detection of hundreds to thousands of nanoparticles; (2) the possibility of wavelength multiplexing.

2. THEORETICAL BACKGROUND

For the theoretical evaluation of the optical behaviour of spherical gold nanoparticles surrounded by a protein layer in different media, we used a Matlab code based on Mie theory [12]. This code is adapted to the two layer model developed by Khlebtsov et al [13] where the nanoparticle with dielectric function $\varepsilon(\omega)$ has a certain diameter and is surrounded by a shell of a certain thickness, and refractive index n_p. This assembly is embedded in a dielectric medium with refractive index n_m. For such a system, the resonance condition is determined by calculating the maximum polarizability.

As we are interested in monitoring the binding of proteins and protein-pairs with layer thicknesses up to 20 nm it is important that the induced dipole field is of sizable amplitude in this range. We have estimated the extension of this field by calculating the change of the resonance condition as a function of the shell thickness, where the shell represents the protein layer bound to the nanoparticle. This was done for various dimensions of the nanoparticle. Results of this calculation are depicted in fig. 2-1a, for a protein layer with n_p=1.5 in a water environment with n_m=1.33. The dielectric function $\varepsilon(\omega)$ of the nanoparticle was adopted from Johnson and Christy [15]. From the figure, it is seen that the resonance conditions of small particles are less sensitive to changes in the layer thickness in our range of interest.

However, the use of a small particle is preferable in view of the relatively small number of protein molecules that can be accommodated on such a particle. Therefore, we decided that a good compromise is the use of 60 nm particles. An additional argument for this choice is the good visibility of these particles in darkfield microscopy.

Another point of interest is the change of the resonance condition as a function of the number of protein molecules bound to a single nanoparticle. To this end, first we considered an imaginary layer of water. The thickness of the layer was taken to be equal to the diameter of a medium sized protein molecule (6 nm). When a protein adsorbs to the surface of the nanoparticle, it replaces an equal volume of water and the effective local refractive index n_{eff} of the layer is changed:

$$n_{eff} = n_m + \frac{N_p}{N_t}(n_m - n_p) \tag{1}$$

where N_p/N_t is the fraction of the covered binding sites. The total number of available binding sites N_t was estimated by calculating the surface area of the nanoparticle and comparing it to the projected area of the protein molecule. Figure 2-1b shows the results of this calculation for a 60 nm nanoparticle.

As we can see, a full layer of proteins (~400 molecules) around the particle would result in a 7 nm shift, which can easily be observed by a spectrophotometer. For a standard spectrometer, capable of 1 nm spectral resolution, we expect that ~50 protein molecules can be detected. In addition, for smaller molecules the detection limit is higher in view of the thinner layer that they will form. The group of Van Duyne [14] was the first to report low-number detection limits.

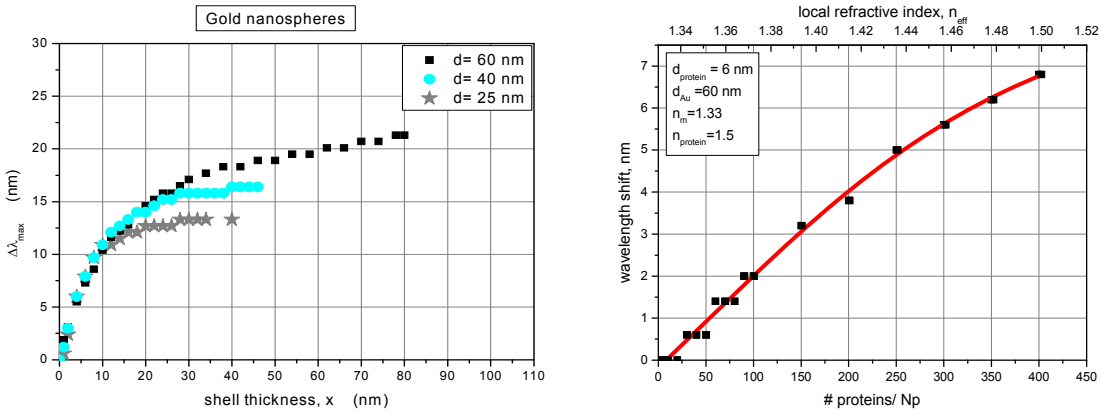

a) b)

Figure 2-1 a) The extension of the sensing volume for nanoparticles of different sizes; b) Expected wavelength shift as a function of the number of adsorbed protein molecules

Although these absolute theoretical detection limits seem quite impressive, it should be realized that in many practical sensor applications the main parameter of interest is the minimum *concentration* that can be detected. The net covered fraction N_p/N_t will be largely determined by the affinity constant of the reaction under consideration. This implies that in this type of applications nanoparticles will only be useful if a large number of identically prepared particles can be simultaneously and individually observed.

3. EXPERIMENTS

3.1 Optical setup

To collect the scattered light from individual gold nanoparticles (images and spectra), we used an inverted Olympus GX71 microscope in a transmission darkfield configuration in combination with a fibre spectrophotometer (Ocean Optics QE65000, 1024x64 pixels).

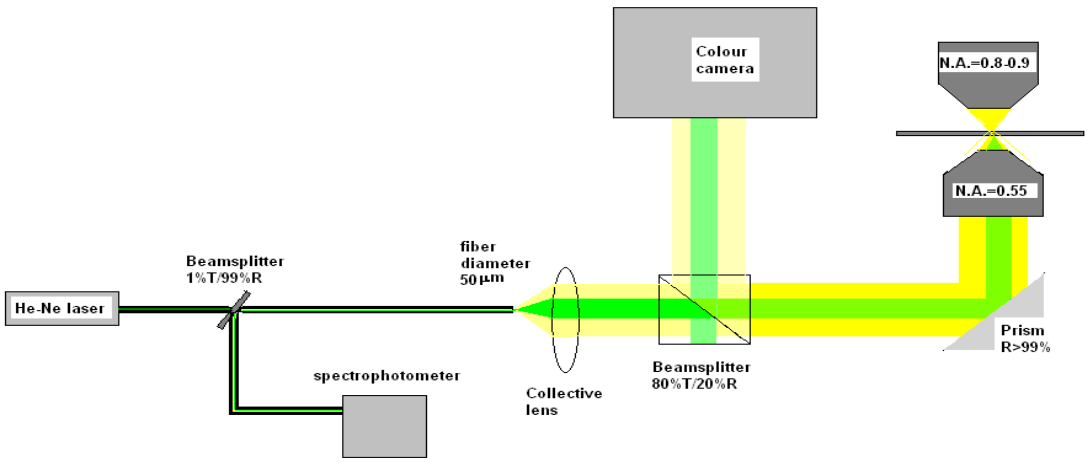

Figure 3-1 Experimental setup

The sample was illuminated from above using a halogen lamp (100W) and focused by a dry darkfield condenser of high numerical aperture (N.A=0.8-0.9). The scattered light of the sample was collected by a UPLANFluor 20x objective (N.A.= 0.55) ; 80 % was sent to the fibre spectrometer, using a 50 µm fibre, and 20% to the colour camera

(Carl Zeiss HRc, 1040x1388 pixels, 14 bits colour depth). The image of a tightly focussed spot produced by a HeNe laser (532 nm) allowed us to select individual nanoparticles for spectral analysis (cf. fig. 3-1). The time required to obtain a single nanoparticle spectrum with sufficient SNR was 50 s, whereas the exposure time to obtain an image with the camera was 250 ms.

3.2 Materials

As a substrate for the sensor chip, we used BK7 coverslips (26mm x 76mm, 0.17 mm thick) purchased from Menzel Glaser, Germany. The gold nanoparticle colloidal solution was purchased from BBInternational (Cardiff, UK). The antibodies used in our experiments, polyclonal anti-biotin antibody (Ab) developed in goat and anti-goat antibody developed in donkey, were provided by Sigma Aldrich.

3.3 Surface modification

Prior to any modification of the glass slides a cleaning procedure was used (Piranha solution (1 H_2O_2 : 3 H_2SO_4 (>96%)) at 95 ^{0}C for 15 min). Immediately after cleaning, the slides were washed with MilliQ water under sonication for 5 minutes. Then the glass slides were dipped in a solution of 10% (3-Aminopropyl)Triethoxysilane (APTES) for 10 minutes and then 5 times washed with MQ water and sonicated each time for 1 minute. Through this procedure, we ensure that the excess of APTES is removed and the layer of the coating is uniformly distributed over the glass surface. Subsequently, the surfaces were baked for 2 hours in an oven at 100^{0}C. This procedure removed all water residues from the surface. After baking the slides were dipped in a gold solution of $1.4 \cdot 10^9$ part/ ml for 5 minutes, resulting in nanoparticle-covered substrate, where the particles had an average distance of ~10μm. The interaction of the nanoparticles and the APTES layer acts through the APTES amino groups and is of electrostatic nature. Although it is a weak interaction, it is sufficient to keep the nanoparticles on the surface both in high flow rates and the high voltages required for Scanning Electron Microscopy (SEM) investigations.

3.4 Antibody modification

As thiols exhibit a high affinity to a gold surface, such a group was conjugated to the anti-goat antibody. To this end a 100 μl Ab solution ($6.7 \cdot 10^{-10}$ mol) was mixed with 100 μl 2-iminothiolane solution ($7.3 \cdot 10^{-7}$ mol) in 700 μl PBS buffer pH 8.7 and was incubated for 120 min under shaking at 4^{0}C and at 250 RPM. The excess of unbound 2-iminothiolane was removed by ultra-filtration. The immunoreactivity of this conjugate towards the antibiotin protein turned out to remain intact, as was apparent from a series of immunoprecipitation experiments (data not shown).

3.5 Data analysis

To analyse the images a custom-made Matlab code was used. The parameter r/g, defined as the ratio between the pixel value of the red channel and that of the green channel, was used as a measure of the colour change of individual nanoparticles. We experimentally demonstrated the invariance of the r/g ratio of a nanoparticle to luminosity changes and colour temperature of the light source. The convincing argument in choosing this parameter was the higher sensitivity to colour change than other evaluated parameters.

This Matlab code allowed us to determine the evolution in time of the r/g ratio for all nanoparticles of interest present in our field of view (FOV) from a series of images. The procedure for determining the r/g consisted of several steps. First, all raw images were background corrected using a digital filter. Then, an image preceding any change in the system is chosen and is defined as reference. A digital mask was applied to this image, to locate and select the particles of interest, based on a selection algorithm. For the selected particles, we have calculated their r/g from the consecutive images and the results were stored in an output file.

The data obtained from the image analysis and the spectra of single nanoparticles were analysed using Origin software.

4. RESULTS AND DISCUSSION

Figure 4-1a shows a darkfield image of *individual* 60 nm particles of a typical sample. Here, the average distance between two nanoparticles is ~10 μm; in our FOV (230x170 μm^2) we expect to have ~400 particles.

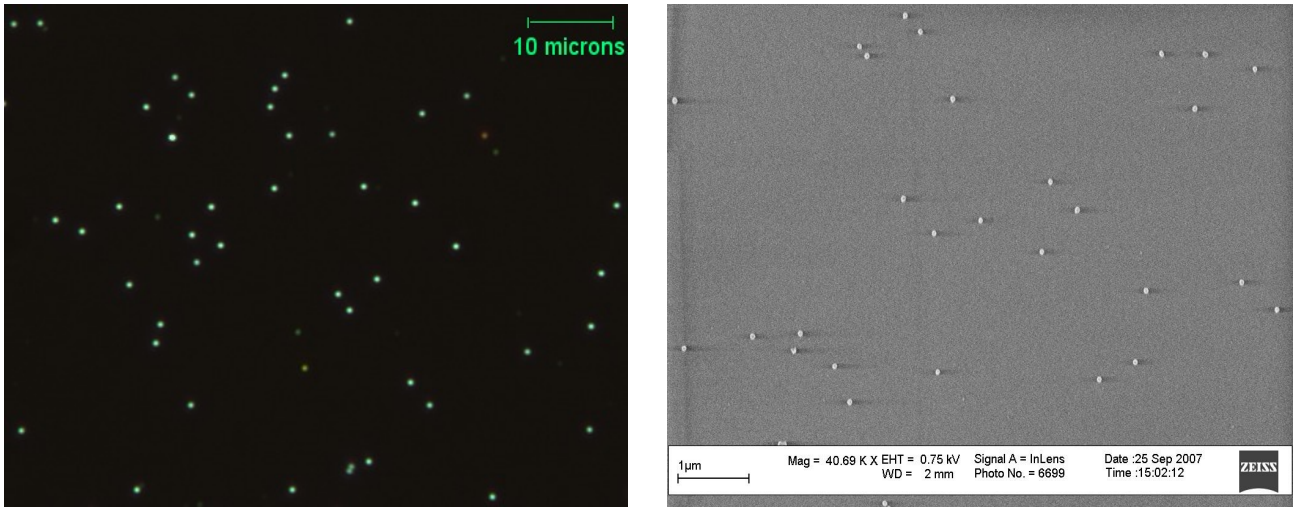

a) b)

Figure 4-1 60 nm Au particles immobilized on glass surface in a) Darkfield microscopy and b) SEM

Figure 4-1b shows a SEM image of 60 nm Au particles with a longer immobilization time showing that at this combination of concentration and immobilization time aggregation does not occur.

4.1 Colour camera as detector for spectral shifts

Theoretically, we determined that we should be able to observe the binding of ~50 proteins of 6 nm diameter to a particle, using a regular spectrophotometer capable of resolving ~1 nm spectral shifts. However, in the present context a major disadvantage of the use of a spectrophotometer is that it is only capable of acquiring a single nanoparticle spectrum at a time.

With the colour camera, this disadvantage is overcome, as we can measure simultaneously the signal from *all* nanoparticles present in the FOV. We performed a series of experiments to find out what is the minimum spectral shift that can be detected by the colour camera.

Firstly, we used transparent solutions with different pH and then we added an amount of pH indicator that changed its colour according to the pH of the solutions. The solutions used in our experiments were selected based on the following criteria:

- their spectra should resemble as much as possible those of the Au nanoparticles used in our experiments;

- the extinction level has to be the same in each solution;

Secondly, experiments were done to check the invariance of the r/g value to the absorption level. We prepared a series of solutions with a certain pH and different extinction levels. The results showed no change in the r/g ratio, as expected.

Thirdly, from all available solutions we selected those showing a 1 nm shift. The results of these experiments, as shown in table 4-1, demonstrate that a colour camera can detect at least 1 nm spectral shift. We did not determine if this is the limiting spectral sensitivity of our colour camera, as we encountered some difficulties in preparing two solutions that have a mutual spectral shift of less than 1 nm.

Table 4-1 pH solutions with 1 nm shift

Sample	λ_{max}(nm)	R (D.N.)	G (D.N.)	B (D.N.)	r/g
1.	511	14937±122	13787±118	13571±117	1.08±0.01
2.	512	15013±123	13430±116	13093±115	1.12±0.01

4.2 Calibration of the camera

Two sets of samples with 60 or 80 nm Au particles immobilized on glass were placed into custom-made flowcells and used for calibration. The initial embedding medium is water. The experiments were done using the optical setup described in section 3-1.

Firstly, we determined the spectra of 10 particles from each set and the results were compared to theory. Figure 4-2 shows typical spectra acquired with the spectrophotometer. From the comparison with simulated spectra, we observe a wavelength shift of a few nanometers. One reason for the difference could be that the nanoparticles used in the experiments have a somewhat other size and/or shape than those used in the simulation.

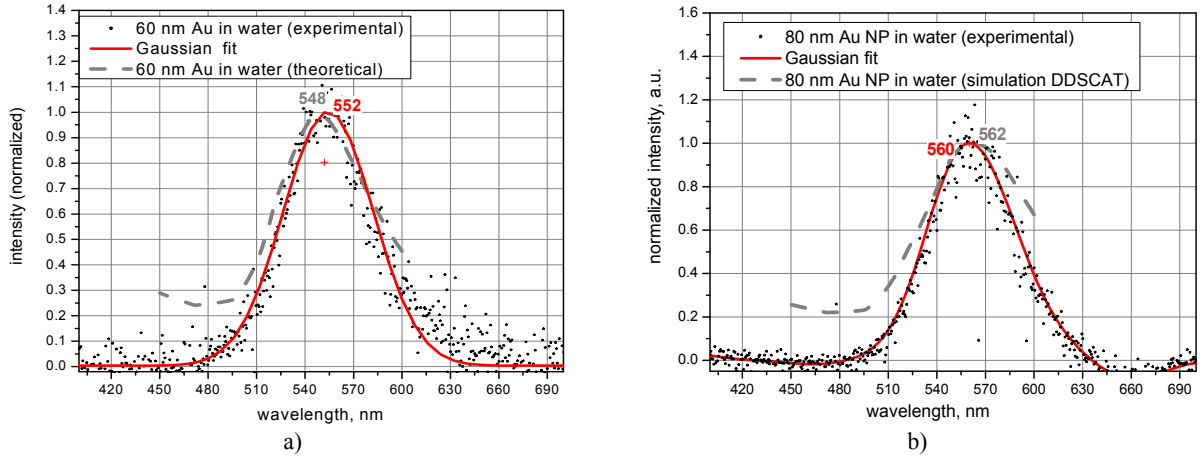

Figure 4-2 A typical spectrum of a) 60 Au particle and b) 80 nm Au particle

Subsequently, the sensor surfaces were subject to changes of refractive index by adding glucose solutions of different concentrations. Each step was followed by washing with MilliQ water.

Two types of information were obtained from these experiments: calibration curves for the colour camera for the two sets of samples and the sensitivity curves for the 60 nm Au particles. Figure 4-3 shows both the experimental and simulated sensitivity curves.

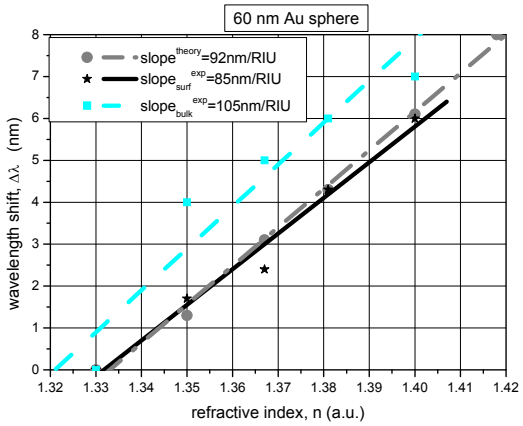

Figure 4-3 The sensitivity curves for 60 nm Au particle determined (●) theoretically, (★) for a single nanoparticle immobilized on surface and (■) for a distribution of particles in bulk solution.

By comparing the theoretical data, obtained in a uniform environment, and the experimental data for the nanoparticle immobilized on glass, we can conclude that the presence of the substrate has a limited effect on the sensitivity behaviour of the nanoparticles. The higher sensitivity slope in the bulk solution could be the result of the size distribution of the nanoparticles present in the solution.

The accuracy in determining the refractive index of the embedding media was $\Delta n = 5*10^{-3}$. The average of 10 separate spectral or r/g measurements was used for further data processing.

The calibration results for the colour camera are shown in figure 3-2 for the two sets of particles. For the refractive index calibration, we determined that the minimum refractive index change that can be detected with 60 and 80 nm Au particles is 10^{-2} and 10^{-3}, respectively. With respect to the wavelength calibration curves for the two sets of nanoparticles, we conclude that the limit of resolution is ~1 nm.

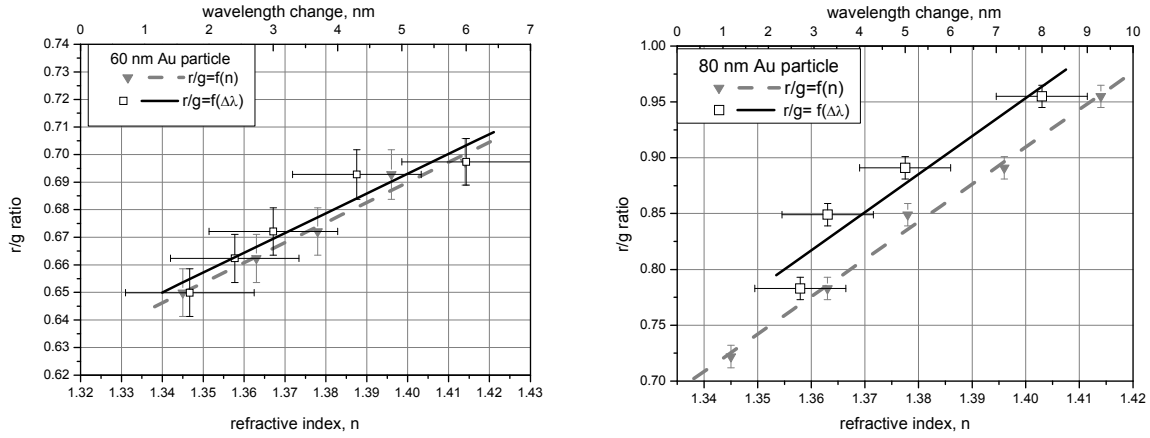

Figure 4-4 The calibration curves for a) 60 Au and b) 80 nm Au particles

Using the arguments presented above, we can conclude that the colour camera can be considered as an alternative method to detect adsorption processes.

4.3 Protein adsorption assay

A simple protein adsorption assay was designed to test this hypothesis. A schematic representation of the experiment is depicted in figure 4-5.

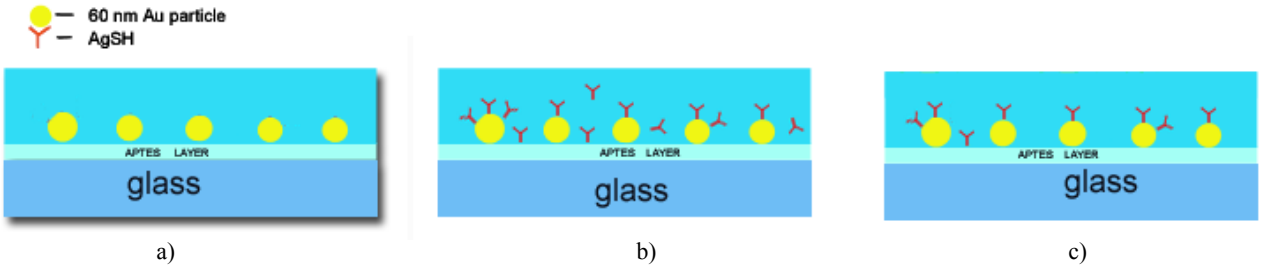

Figure 4-5 Schematic representation of the protein assay. The surface chip (a) is incubated for 45 minutes with thiolated anti-goat antibody (AgSH) (b) and then washed (c) with MilliQ water

A flowcell containing a sensing surface with 60 nm Au particles was used for the protein assay. The flowcell is divided in three channels of which two were used: one for the control, where no antibody is added and one for the adsorption experiment. The control experiment was done later, as we were limited in observing only one channel at a time. The images were acquired at 1-minute intervals.

Initially, both channels were rinsed with MilliQ water for 5 minutes at a flow rate of 4.2 µl/min. Then, in the experiment channel, we introduced the thiolated antigoat (AgSH, $5*10^{-8}$M) for 45 minutes to adsorb on the surface of the nanoparticle, while in the reference channel we continued to add MilliQ water. The last step of the experiment is the washing of the channels with MilliQ water.

The results are shown in figures 4-6, 4-7a and 4-7c. They represent only a small part of the total amount of available data. Particles with no significant signal change were also present. A possible explanation for this could be that the binding sites of those nanoparticles were blocked before the start of the experiment.

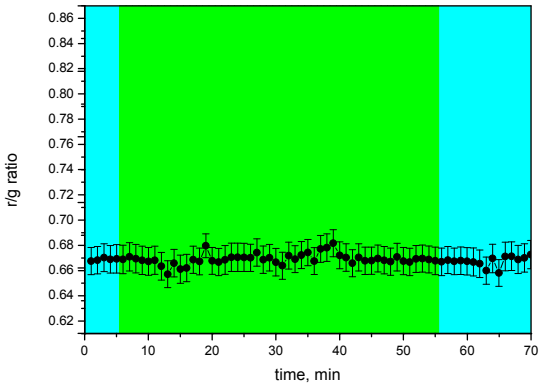

Figure 4-6 A typical signal from one nanoparticle in the control experiment

By combining the results from the control, figure 4-6, and the assay experiments, figure 4-7a and 4-7c, we can conclude that the increase of the signal can only originate from the protein binding to the particle's binding sites.

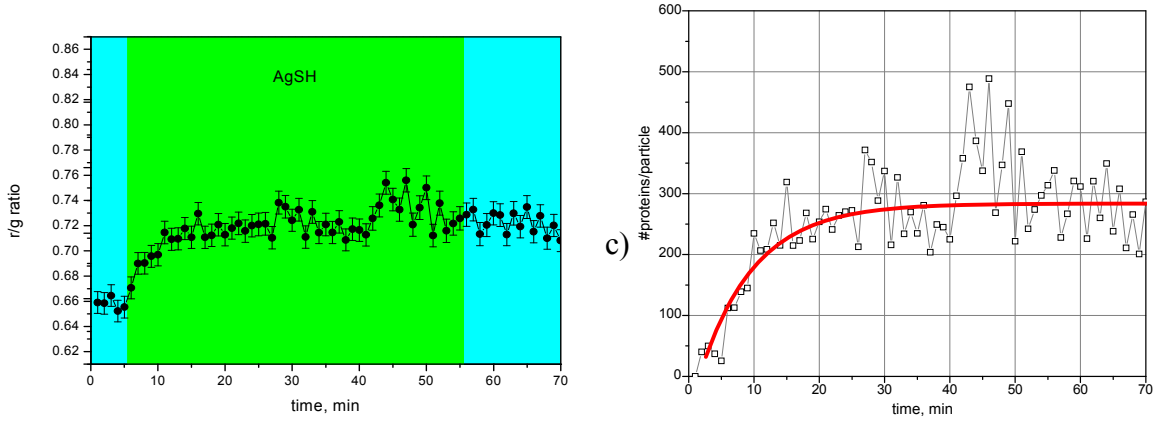

a) b)

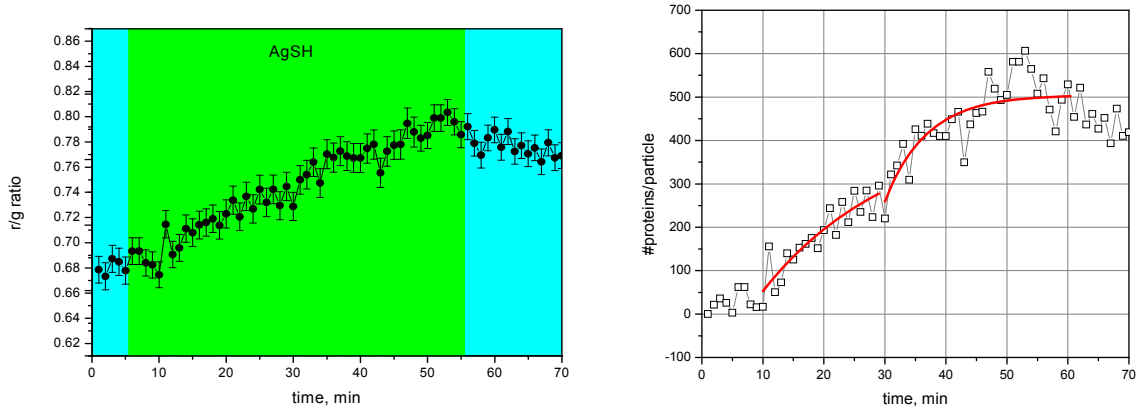

c) d)

Figure 4-7 The raw and quantified curves a), b) and c), d), respectively, of two different signals. At t=1-5min the sample was rinsed with MilliQ water then at t= 6-55 min AgSH was added and washed again with MilliQ water (t= 56-70 min).

The signal from figure 4-7a has the profile of a characteristic binding curve of a protein. In the time intervals, 28-30 minutes and 43-52 minutes, two larger signal increases were observed, which disappear after a while. A possible explanation for this could be that impurities from the external environment entered in the protein solution and immobilized near the nanoparticle; at a random time, they re-entered the flow and were washed away. In this signal, no visible dissociation process is observed in the washing step.

Figure 4-7c shows a different type of behavior. The evolution of the signal until t=30min shows a binding curve with a slower rate than the previously discussed signal. Starting at t=31min, the development of a second curve suggests that a second layer of protein was formed which, however, appears to be removed in the washing step starting at t=56 min.

4.4 Quantification

For the quantification of the occupied binding sites of the particle, we combined the experimental data with the calibration and theoretical curves presented in figure 4-4, and figure 2-1b. In figure 4-7b and 4-7d is illustrated the quantification of the two measured binding curves. While figure 4-7a shows a clear saturation level at ~300 molecules, figure 4-7d shows the formation of a second binding curve on top of the 300 molecules level. This emphasizes the observation that for the formation of a complete layer of protein on the 60 nm Au particles ~300 molecules are necessary.

5. CONCLUSIONS

In summary, this work shows the feasibility of using the colour camera for the measuring of a kinetic process and its quantification.

By proving its feasibility, the use of a colour camera shows a clear advantage over the current spectroscopic detection methods, as it can perform a parallel measurement of the optical properties of all nanoparticles present in the FOV. Additionally, quantification in terms of concentrations might be determined. However, the sensitivity of our method using the current type of assay is not sufficient for many practical sensor applications. To this end, the introduction of an alternative type of assay, based upon the wavelength shift of approaching nanoparticles seems more adequate [9].

In addition, the concept of the detection method presented in this paper provides an outlook to its use in wavelength multiplexing sensing.

6. ACKNOWLEDGEMENTS

We thank Aufried Lenferink for his technical support.

This research was financially supported by MicroNed (project nr. WP2F-FoAc) and by the European Union (FP6 STREP Project Fluoromag (Proj. nr. 037465)).

REFERENCES

[1] Nath, N., Chilkoti A., "Label Free Colorimetric Biosensing Using Nanoparticles", Journal of Flourescence, Vol 14, No.4, 377-389, (2004)

[2] Schultz S., Smith D. R., Mock J. J., Schultz D.A., "Single –target molecule detection with nonbleaching multicolor optical immunolabels", PNAS, vol.97 , no.3, 996-1001, (2000)

[3] Fritzsche W., Taton T.A., "Metal nanoparticles as labels for heterogenous chip-based DNA detection", Nanotechnology 14, R63-R73, (2003)

[4] Okamoto T., Yamaguchi I., Kobayashi, T., "Local plasmon sensor with gold colloid monolayers deposited upon glass substrates," Opt. Lett. 25, 372-374 (2000)

[5] Anker J. N., Hall W. P., Lyandres O., Shah N. C., Zhao J., Van Duyne R. P., "Biosensing with plasmonic nanosensors", Nature materials, vol.7, 442-452, (2008)

[6] Yonzon, C. R. et al., "Towards advanced chemical and biological nanosensors — an overview", Talanta 67, 438–448 (2005).

[7] Haes, A. J., Chang, L., Klein, W. L. & Van Duyne, R. P., "Detection of a biomarker for Alzheimer's Disease from synthetic and clinical samples using a nanoscale optical biosensor", J. Am. Chem. Soc., 127, 2264–2271 (2005).

[8] Chen, Y., Munechika, K. & Ginger, D. S., "Dependence of fluorescence intensity on the spectral overlap between fluorophores and plasmon resonant single silver nanoparticles", Nanoletters. 7, 690–696 (2007).

[9] Sannomiya T., Hafner C., Voros J., "In situ sensing of single binding events by localized surface plasmon resonance", Nanoletters, 8(10): 3450-3455,(2008)

[10] Baciu C.L., Becker J., Janshoff A., Sonnichsen C., "Protein- Membrane Interaction Probed by single plasmonic nanoparticles", Nanoletters, Vol.8(6), 1724-1728, (2008)

[11] Yguerabide J., Yguerabide E., " Light-scattering submicroscopic particles as highly fluorescent analogs and their use as tracer labels in clinical and biological applications-theory", Analytical Biochemistry, 262, 137-156, (1998)

[12] Matzler C.,http://www.iwt-bremen.de/vt/laser/wriedt/New/new.php3

[13] Khlebtsov N. G. ,Dykman L. A.,Bogatyrev V. A., Khlebtsov B. N., "Two-Layer Model of Colloidal Gold Bioconjugates and Its Application to the Optimization of Nanosensors", Colloid Journal, vol 65, no 4., (2003)

[14] McFarland A., Van Duyne R. P., "Single silver nanoparticles as real –time optical sensors with zeptomole sensitivity", Nanoletters, Vol3(8), 1057-1062, (2003)

[15] Johnson P., Christy R.," Optical Constants of the Noble Metals" Phys. Rev. B6 , p. 4370 - 4379, (1972)